

# Intelligent scheduling of urban drainage systems: effective local adaptation strategies for increased climate variability

Kun Xie<sup>1</sup>, Jong-Suk Kim<sup>1</sup>, Linjuan Hu<sup>2\*</sup>, Hua Chen<sup>1\*</sup>, Chongyu Xu<sup>3</sup>, Jung Hwan Lee<sup>4</sup>, Jie Chen<sup>1</sup>, Sun-Kwon Yoon<sup>5</sup>, Di Zhu<sup>1</sup>, Shaobo Zhang<sup>1</sup>, Yang Liu<sup>1</sup>

1. State Key Laboratory of Water Resources and Hydropower Engineering Science, Wuhan University, Wuhan 430072, China.
  2. Water Resources Bureau of Chenzhou, Hunan 423000, China
  3. Department of Geosciences, University of Oslo, Norway.
  4. Water Resources Management Research Center, K-water Research Institute, Daejeon 34350, South Korea.
  5. Department of Safety and Disaster Prevention Research, Seoul Institute of Technology, Seoul 03909, South Korea.
- \* Corresponding author: Hua Chen(chua@whu.edu.cn) ; Linjuan Hu(517182250@qq.com)

## Abstract

Intelligent scheduling of urban drainage systems is generally regarded as a potentially sustainable strategy for urban flood management. To investigate the effectiveness of the intelligent scheduling strategy in mitigating urban flooding, a new intelligent scheduling model (ISM) that couples the Storm Water Management Model (SWMM) and a multiobjective particle swarm optimization algorithm is proposed for a simulation-optimization framework. The objectives of the ISM are to minimize the flooding volume, front-pool water level fluctuation, and operational cost. Synthetic rainfall events with different durations and return periods based on the Gumbel distribution and observed rainfall events are utilized to comprehensively assess the designed model's performance in the Dealim3 catchment, South Korea. The selected ISM-based scheduling strategies are assessed in accordance with climate change mitigation (i.e., reducing greenhouse gas emissions) and local adaptation (i.e., improving drainage systems). The results indicate that these strategies generated by ISM lead to reductions in flooding, water level fluctuation, and operational costs. The maximum daily rainfall with a 100-year return period increased by 2.1% and 6.8% during 2025-2064 under SSP1-2.6 and SSP5-8.5, respectively, compared with the historical period (1975-2014), thereby increasing the magnitude of urban flooding. The ISM may also significantly lower the flooding process at specific nodes. The ISM-based strategy outperforms climate change mitigation and other adaptation strategies. This study shows that the ISM-based strategy are very useful to deal with the impact of climate change on urban flooding.

**Keywords:** urban drainage system; urban flooding; simulation optimization; adaptation strategy; mitigation strategy

# 1. Introduction

Urban flooding can cause fatal, adverse impacts on city services and the environment, with socioeconomic implications (Lund et al. 2020; Mahmoud and Gan 2018). The most crucial factor contributing to urban flooding events is climate change, which may lead to increased flood frequency and magnitude (Mahmoud and Gan 2018). The urban drainage system (UDS), an essential part of city infrastructure that collects, transports, and stores wastewater and stormwater, has enormous economic and environmental impacts (García et al. 2015). However, historically designed urban drainage systems cannot carry the additional load caused by climate change (Ghodsi et al. 2020), resulting in the overflow of storm sewer systems (Lund et al. 2019). Therefore, future drainage systems must consider the growing frequency and intensity of rainfall to enable appropriate responses to variable circumstances.

Many studies have demonstrated the impact of climate change on urban flooding. Methodologies for reducing urban flood damage under climate change have been explored, including climate change mitigation and adaptation strategies (Zhou et al. 2018; 2019). Zhou et al. (2018) used RCP 8.5, representing the business-as-usual scenario, and RCP 2.6, representing the climate mitigation scenario, to examine the benefits of climate mitigation in reducing flood volumes. The result of climate mitigation was compared

with the adaptation scenario (expanding the drainage system). These researchers suggested that the local adaptation strategy was more effective in reducing flood volumes than the mitigation strategy. Adaptation strategies such as applying low-impact development (LID) measures or expanding facilities are the typical measures taken (Zhou et al. 2018). However, these measures generally involve high costs or need extra space, making these solutions impracticable in some cases.

Other alternatives are related to the scheduling strategy, which can adapt to upcoming situations and fully use the drainage capacity and storage of existing drainage systems (Wong and Kerkez 2018). Traditionally, the scheduling rules of the pump station or orifice mainly depend on expert experience, which were set up a long time ago and cannot cope with urbanization and climate change. Employing updated scheduling strategies that can replace the static operation rules with dynamic rules on the existing drainage facility brings flexibility to the mitigation of urban flooding without extra investment in infrastructure expansion or occupation in urban areas (Lund et al. 2019; Rathnayake and Anwar 2019).

The problem in drainage systems scheduling is usually multi-objective (Yang et al. 2019), uncertain (Meng et al. 2020), and dynamic (García et al. 2015). Urban water systems need to be scheduled by multi-objective dynamic scheduling rules to take advantage of the storage and conveyance capacity of

existing facilities to enhance the performance of the water system. Furthermore, the multiobjective optimization model has been extensively explored. For instance, Sadler et al. (2019) considered minimizing the flooding and the deviation from the target water depth at the storage unit; Yang et al. (2019) included the water level fluctuations in the flood storage pond (FSP), the peak FSP water level and the difference in pump switches between two continuous times. However, these studies found the best scheduling rules via the multiobjective weighted sum method, transferring the multi-objective into a single objective, which cannot balance the trade-off benefit among objectives along the Pareto front (Das and Dennis 1997).

For flood control, simulation-optimization methods have been used in urban drainage systems (Hsu et al. 2013). The one-dimensional hydrologic-hydrodynamic SWMM model (Rossman, 2009) is commonly used to simulate urban floods caused by overflows in urban drainage systems (Wang et al. 2021; Zhou et al. 2019). Wang et al. (2021) proposed a sluice control scheme to minimize flooding and water depth based on an offline optimization system by coupling the SWMM model with a differential-evolution algorithm. Zhou et al. (2018) confirmed that SWMM has the potential to evaluate the performance of drainage systems under mitigation and adaptation scenarios. However, few studies have comprehensively compared the performance of scheduling strategies based

on simulation-optimization methods with climate change mitigation and local adaptation strategies. So, this study aims to design a multiobjective intelligent scheduling model (ISM) in the simulation-optimization framework by coupling the SWMM model with the multiobjective particle swarm optimization algorithm (MOPSO), which is helpful to find better effective solutions to cope with the multiobjective scheduling problem.

To comprehensively explore which strategy is more effective, the performance of ISM in mitigating urban floods, improving infrastructure stability, and minimizing operational cost are also compared with other local adaptation strategies (i.e., installing LID and expanding facilities) and climate change mitigation strategy under various rainfall events, which could promote decision-making and generate an efficient and economical optimal scheduling rule for the actuators of the urban drainage system. To our knowledge, this is the first study designing an ISM-based adaptation strategy and comparing its performance with climate change mitigation and local adaptation strategies to find the best strategy in mitigating urban floods, improving infrastructure stability, and lowering operational cost under changing climate in Seoul, South Korea. Detailed information on the various strategies is provided in Supplementary Information S4.

## 2. Material and Methods

### 2.1 Study area and data

The Dorim stream, a branch of the Han River in Seoul, South Korea, often suffers inundation in the wet season due to the insufficient capacity of an urban drainage system designed for historical conditions. Therefore, the Dealim3 catchment located in the Dorim stream watershed is selected as the study area. The urban drainage system of the Dealim3 catchment (Fig. A1) consists of a detention reservoir, three pump stations (Daerim2, Daerim3, and Daerim DR), front pools, a weir, and a pipe network. The detailed information of these components can be found in Table A1. The current operation rules of all pump stations designed by the previous study are utilized (Ngo et al. 2016). The detailed SWMM model in the Daerim3 catchment refers to Lee et al. (2020).

To verify and assess the performance of the designed ISM in the simulation-optimization framework, synthetic rainfall and historical rainfall events with different durations and return periods are utilized (Supplementary Information 1). The flow time series at the Daerim2 and Daerim3 pump stations are supplied to calibrate and validate the SWMM model. The rainfall events with ten-minute intervals monitored by the AWS 410 automatic weather station and flow series from 21:30 on September 20, 2010, to 5:50 on

September 22, 2010, are collected to calibrate the model. The corresponding data from July 26, 15:40 to July 29, 16:20 in 2011, are used for model validation. For detailed information on model calibration and validation, refer to Supplementary Information 2.

## **2.2SWMM model**

SWMM can execute a single event or continuous simulation of runoff in urban areas, including river channels, pipe networks, sluices, pumps, and weirs. The simulation area is divided into several homogeneous subcatchments, which generate runoff and pollutant loads after receiving precipitation. After slope confluence, the routing portion is carried out in the pipes, channels, storage devices, and actuators (pump, weir) until the outlet of the drainage area is reached. The model is generalized as a nonlinear reservoir in each subcatchment area to calculate the surface runoff. The routing portion of the pipeline or channel is based on kinematic waves or dynamic waves. Generally, the SWMM can simultaneously meet the requirements of hydrology, hydraulics, and water quality simulation. During simulation, the SWMM can track the flow and depth of the pipe and channel and the overflow of the manhole for each time step.

In this study, the nonlinear reservoir method is applied to model overland flow routing. Horton's method is used to compute the infiltration losses. A



dynamic wave is selected to simulate the routing of conduit flow. Since the SWMM cannot simulate surface inundation dynamics, flood conditions are reflected by the overflow at the manhole (Zhou et al. 2018). Once surface runoff exceeds the capacity of drainage systems, the overflow expressed as total flood volume (TFV) occurs.

### 2.3 Multi-Objective Particle Swarm Optimization algorithm (MOPSO)

Particle swarm optimization (PSO) (Kennedy and Eberhart 1995) is a kind of adaptive probabilistic optimization technology that simulates the intelligent behaviour of a swarm. It begins with random initialization and searches for the optimal solution through an iterative process. Evaluating the quality of solutions is based on fitness. In PSO, each particle has two state vectors, as shown in Eq. (1) and Eq. (2): position vector (the decision variable) and velocity vector. PSO has attracted much attention because of its superiority in solving practical problems such as easy implementation, unique searching mechanism, and fast convergence (Yang et al. 2009).

$$v_i^t = w^t v_i^{t-1} + c_1 r_1 (pbest_i - x_i^{t-1}) + c_2 r_2 (gbest_i - x_i^{t-1}) \quad (1)$$

$$x_i^t = x_i^{t-1} + v_i^{t-1} \quad (2)$$

$$w^t = w_2 + (w_1 - w_2) \times (M - t) / M \quad (3)$$

where  $v_i^t$  is the velocity vector,  $w^t$  is inertia weight,  $c_1$  and  $c_2$  is an acceleration factor,  $r_1$  and  $r_2$  is a random value between [0,1],  $pbest_i$  is the

personal optimum,  $gbest_i$  is the global optimum at generation  $i$ ,  $x_i^t$  is the position vector,  $i$  is the number particle,  $w_1$  is initial inertia weight,  $w_2$  is the inertia weight when iterating to the maximum number,  $t$  is the current number of iterations and  $M$  is the maximum number of iterations. In this study, linear decreasing inertia weight is used, which is expressed in Eq.(3).

In reality, many problems have multiobjective functions; PSO has been extended to satisfy the actual demand, and multiobjective particle swarm optimization (MOPSO) has been proposed (Mostaghim and Teich 2003; Yang et al. 2009). In MOPSO, the global optimal solutions are nondominated solutions; choosing the global optimal particle and personal optimal particle from Pareto-optimal solutions is difficult. Furthermore, the niche sharing mechanism (Liu et al. 2006; Bi and Wang 2018) and roulette wheel selection are used to solve the global optimal particle. The calculation process of MOPSO is shown in Fig. A2. More information on the niche-sharing mechanism is provided in Supplementary Information 3.

## **2.4 Multiobjective optimization scheduling model**

In this study, pump stations and weirs play a decisive role in urban inundation control systems and urban drainage systems (Jafari et al. 2018; Ngo et al. 2016; Yazdi et al.2016), which can fully utilize the storage capacity and conveyance capability of drainage systems to avoid flooding. Developing

the optimal scheduling strategy for the pumping station and weir can significantly mitigate the consequences of local flooding. The maximum capacity of the drainage system is  $0.1229 \text{ m}^3$ . However, due to the complex topology of the drainage system, the inflow of the drainage system exceeds  $0.0924 \text{ m}^3$ ; localized flooding occurs through the manhole. The drastic fluctuation of the front pool (inlet of pump stations) water level could cause severe damage to the stability of drainage facilities. The highest front-pool water level has been used as an indicator to reduce inundation risk. However, the fluctuation of the front-pool water level during the operation process is seldom considered a direct indicator for improving the stability of drainage infrastructure. The operational costs of the pump station and weir include the cost of maintaining the machine and the cost of pumpage. The maintenance cost is concerned with the frequent switch on/off of the machine. In fact, the pumpage cost triggered by electric power or diesel fuel runs for only a few hours during a rainfall event. Therefore, the operational cost ( $F_3$ ) is indicated by the maintenance cost of the pump station and weir, which is calculated by the frequency of switch on/off of the pump and weir (Hsu et al. 2013; Yazdi et al. 2016; Yang et al. 2019). Finally, the ISM in the simulation-optimization framework is constructed; three objective functions are included: TFV minimization, front pool water level fluctuation minimization, and operational cost minimization. MOPSO is applied to search the Pareto solutions that

produce trade-offs among the objectives.

Therefore, a multi-objective function is formulated to minimize the TFV ( $F_1$ ), minimize the water level fluctuation of the front pool ( $F_2$ ), and minimize the operational cost ( $F_3$ ) at the whole control horizontal in the study area. The function is expressed as:

$$\left\{ \begin{array}{l} \text{Min}F_1 = \sum_{k=1}^{\text{num}} \sum_{t=2}^T q_{k,t} \\ \text{Min}F_2 = \sum_{j=1}^{\text{sec}} \sum_{t=2}^T |W_{j,t} - W_{j,t}| \\ \text{Min}F_3 = \sum_{i=1}^N \sum_{t=1}^T NP_{i,t} \end{array} \right. \quad (6)$$

where  $t$  is the time instant, the  $q_{k,t}$  is the overflow of manhole and river,  $W_{j,t}$  is the water level of front-pool,  $NP_{i,t}$  is the number of the switch on/off of the pump,  $N$  is the number of the pump station,  $T$  is the number of time steps,  $\text{sec}$  is the number of river cross-section,  $\text{num}$  is the number of manhole occurring overflow. The constraint of the functions refer to Appendix C1.

The switch on/off of the pump or the opening settings of the weir is based on the water depth of the inlet. The scheduling of the weir determines the opening at a specific water level with 0.1 m increments ranging from 0-1.1 m (Ngo et al. 2016). The water level of each pump's switch on/off and the opening settings of the weir at each specific water level are selected as the decision variables corresponding to particles in MOPSO to form a scheduling strategy for the drainage system. The ISM for three pump stations and a weir

includes 45 decision variables.

## **2.5 Coupling of SWMM model and multiobjective optimization scheduling model**

The SWMM is coupled with multiobjective ISM based on MOPSO in the simulation-optimization framework (Fig. A2). The routing process involves the following steps: first, the decision variables are initialized in MOPSO and fed into the SWMM inp file as the scheduling rules of the pump stations and weir; second, the simulation module in MATLAB drives the new SWMM with a new inp file to run and generate the desired results by the EXE file, i.e., the number of pump switches on/off, the water depth of the inlet and the node flooding at each time step; third, the objective function is calculated based on the desired results in the binary file read by the constructed module; finally, updated decision variables generated by MOPSO are fed into the SWMM to obtain the new results. The above procedures are repeated until the stop criterion is satisfied.

## **2.6 Synthetic rainfall events**

To respond to extreme storm events, synthetic rainfall generated artificially under different return periods and durations is selected as the boundary condition of the SWMM. To estimate the synthetic storm of various return periods and durations, the Gumbel distribution and probability-weighted moment (PWM) method used to estimate the parameter of Gumbel is

recommended (Lee et al. 2020; Ryu et al. 2014). The statistical analysis of extreme storms is based on the maximum 10-minute precipitation amount for the Seoul station. In addition, the third quartile of the Huff method (Huff, 1967) representative distribution in Korea is used to generate rainfall distributions for different return periods and durations (Feng et al. 2020). Kolmogorov–Smirnov and Anderson–Darling tests are used to test the goodness-of-fit of the Gumbel distribution at a 95% confidence level.

$$f(x) = \frac{1}{\alpha} \exp\left[-\frac{x-x_0}{\alpha} - \exp\left(-\frac{x-x_0}{\alpha}\right)\right], \quad -\infty < x < \infty \quad (7)$$

$$F(x) = \exp\left[-\exp\left(-\frac{x-x_0}{\alpha}\right)\right] \quad (8)$$

where  $x_0$  and  $\alpha$  are the location and scale parameter, respectively.

The extreme quantiles, known as return level  $Z_p$ , is estimated corresponding to the return period

$$Z_p = x_0 - \alpha \log(-\log(1-P)) \quad (9)$$

where  $P$  is the probability of occurrence, the reciprocal of the return period

$$P = \frac{1}{T} \quad (10)$$

The local adaptation strategies (including the optimal scheduling strategy generated by ISM, the existing facility upgrading strategy, and the simplified LID strategy) and climate change mitigation strategy are employed to compare and analyze the best approach for preventing urban flooding. For detailed information on climate change mitigation and other local adaptation strategies, refer to Supplementary Information 4.

### **3. Results**

#### **3.1 Operation strategy based on the ISM**

Three solutions within the Pareto solutions (Fig. A3) obtained by the designed ISM under different rainfall events and historical events are selected to analyse the performance of the ISM. The strategy with a minimum value of flooding, water level fluctuation, and operational cost in each event is selected to reveal the performance of the designed ISM. The performance assessment is based on the comparison between the result of the selected strategies and the result of the current operation rule. In the current operation rule, a log-linear relationship (Fig. A4) can be discovered to characterize the change in flooding with the increase in rainfall intensity indicated by the return period in this study.

##### **3.1.1 Performance of ISM driven by synthetic rainfall events**

The flooding, water level fluctuation, and operational cost of the optimal scheduling strategy derived by the multiobjective ISM under different rainfall events are different from the current operation rules (Fig. 1).

For the optimal scheduling strategy with minimum  $F_1$ , the flooding reduction is most significant for the different durations and return periods of rainfall events with a 1-7% reduction ratio. Moreover, the water level fluctuation and operational cost change range from 8% to 41% and 79% to 99%, respectively,

compared to current operation rules. The results show that the ISM's optimal scheduling strategy with minimum  $F_1$  can reduce flooding, water level fluctuation, and operational cost, especially operational cost. The flooding, water level fluctuation, and operational cost of the optimal strategy are less than those of the current operation rule.

For the optimal scheduling strategy with minimum  $F_2$ , the operational cost within 97% of strategies in Pareto solutions generated by ISM is decreased. Thus, most strategies obtained by the ISM for various synthetic rainfall events may dramatically reduce the operational cost and flooding, except for the strategy under six-hour duration and 50-year return periods, which can be discarded in the decision-making process. In this particular case, the 62% strategies in Pareto solutions generated by ISM can abate flooding, revealing that the strategies generated by ISM may effectively mitigate flooding. However, flooding from events with a one-hour duration exceeds the current operation rule. The result illustrates that in rainfall events with short durations, lowering water level fluctuations may increase flooding. Therefore, the optimal scheduling strategy with minimum  $F_2$  is more appropriate for long-duration events when considering multiple objectives.

For the optimal scheduling strategy with minimum  $F_3$ , the operational cost can be reduced by more than 97% for all synthetic rainfall events. Furthermore, the water level fluctuation reduction is also improved (23%-71%). The results



demonstrate that an optimal scheduling strategy with minimum  $F_3$  can significantly lower the operational cost and may reduce the water level fluctuation and perform better in more extended duration events for mitigating flooding.

<Fig. 1>

### 3.1.2 Performances driven by observed rainfall scenarios

In the optimal operation strategy with minimum  $F_1$ , the TFV, water level fluctuation, and operational cost are reduced by 13-38%, 17-54%, and 97-99%, respectively. This phenomenon shows that maximum TFV reduction by the intelligent scheduling strategy can also reduce water level fluctuation and operational cost compared to the current operation rule in the observed rainfall scenarios.

For the optimal operation strategy with minimum  $F_2$ , the maximum reduction of water level fluctuation can be achieved with a range of 56-75%. As a result, the operational cost decreased dramatically, ranging from 70% to 99%. However, the TFV increased by 681% and 12% compared to the current operation strategies for scenarios S3 and S4, respectively, these strategies can be treated as abnormal ones. Nevertheless, the ISM is acceptable for S3 and S4 scenarios, though due to flooding, 86% and 81% of the strategies in the Pareto solutions generated by ISM are declined, respectively.

A maximum operational cost reduction of nearly 100% can be achieved in

the optimal operation strategy with minimum  $F_3$  for all rainfall scenarios. In addition, the water level fluctuation and operational cost are reduced by approximately 3-35% and 53-63%, respectively, compared to the TFV of the current operation rule.

### **3.2 The future changes by coupling climate change scenarios**

As shown in Fig. 2(a), the rainfall of the multimodel ensemble means during 2025-2064 for SSP1-2.6 and SSP5-8.5 under different return periods is higher than that in the historical period (1975-2014), increasing by 2.1% and 6.8% for a 100-year return period, which means that future climate change will result in an increase in rainfall. Due to climate change, the TFVs of both the SSP1-2.6 and SSP5-8.5 scenarios increased compared with the baseline scenario in the ranges of 6.7-8.5% and 17.7-27% (Fig. 2(b)), respectively, under different return periods. Moreover, the flooding of SSP5-8.5 is higher than that of SSP1-2.6. The flooding uncertainty based on the SWMM and CMIP6 also increases as the rainfall intensifies (return period). For water level fluctuation (Fig. 2(c)), no noticeable regular increase or decrease can be found in SSP1-2.6 and SSP5-8.5, with ranges of -14.5% ~ 3.3% and -14.2% ~ 11%, respectively. Under the climate change scenarios, the operational cost (Fig. 2(d)) is greater than that under the baseline scenario and increases with the rainfall intensity.

<Fig. 2>

### **3.3 Comparison of the different strategies**

#### **3.3.1 TFV, water level fluctuation, and operational costs**

The optimal strategy with minimum flooding generated by the ISM, climate change mitigation strategy, infrastructure upgrade strategy, and simplified LID strategies are applied to compare the performance of reducing flooding, improving infrastructure stability, and decreasing operational cost. The reduction rate compares each strategy with the current operational rule (baseline scenario). The flooding, water level fluctuation, and operational cost reduction of different strategies compared to the results of the current operation rule are revealed in Fig. 3.

The flooding reduction ratio increases with increasing DR detention, ranging from 55-100%, 32-81%, 25-66%, and 18-41% for return periods of 10, 30, 50, and 100 years, respectively. However, the rate of increase slows with increasing DR detention. The flooding reduction of rainfall events with a ten-year return period is nearly 100% for 20% enlarging scenarios. In addition, the water level fluctuation of the detention enlarging scenarios is higher than that of the baseline scenario (4-16%). The total cost of the DR detention enlarging scenario, including the material, construction and operational costs, is more expensive than the baseline scenario, even though the operating cost is similar.

The flooding reduction is enhanced with the ratio of surface permeation, in which increased runoff can be contained with the more permeable areas and is less than the rainfall intensity. Furthermore, the simplified LID strategies could potentially reduce TFV by approximately 22-62% for different rainfall events. The different flooding reductions among different rainfall events can be discovered for the same simplified LID scenario, demonstrating that the LID strategy is more adapted to different rainfall events. The water level fluctuation reduction is less than that of the ISM strategies. Reducing impervious surfaces will also lower the operational cost of the facility.

The climate change mitigation strategy represents the worst scenario, with the most negligible flooding reduction and the highest water level fluctuation. The strategy generated by ISM results for the most significant reductions in flooding, water level fluctuation, and operational cost under all rainfall events fell within ranges of 46-100%, 55-86%, and 99-100%, respectively. Furthermore, the flood reduction decreased with the increase in return periods. The comparison result demonstrated that the strategy generated by ISM could effectively mitigate flooding, improve infrastructure stability, and lower operational costs, especially for lower operating costs nearly doubled.

<Fig. 3>

### 3.3.2 Flooding time series at a specific node

Fig. 4 shows the results from different control strategies under different synthetic rainfall events with 1440 minutes duration. Flooding occurs when the water depth at a specific node exceeds the maximum depth of the node. The series flooding node MH23446 is selected as the focus node to describe the flooding process of external extreme rainfall events. With the increase in return periods of the rainfall events, much more flooding occurs.

In the intelligent scheduling strategy, flooding is eliminated under rainfall events with 10 and 30 return periods. The flooding is negligible, with a flooding peak of less than  $0.2 \text{ m}^3/\text{s}$  under rainfall events with 50 and 100 return periods. The ISM also delays the flooding peak time. The results imply that the ISM may effectively mitigate flooding at the severe flooding node.

As detention expands, less flooding occurs at the specific node, and the flooding peak is also gradually reduced. However, flooding cannot be eliminated due to insufficient storage available to handle the substantial amount of flow, and the detention unit is still overtopped. Additionally, the impact of improving impervious surfaces on lowering flooding is similar to the increase in detention. Climate change will increase flooding at MH23446. The climate change mitigation strategy may reduce flooding, though it performs worst in mitigating flooding.

<Fig. 4>

## 4. Discussion

### 4.1 Performance of the ISM-based strategy

The results of different rainfall events confirm that the multiobjective ISM can generate an effective operation strategy for pump stations and weirs by utilizing the storage and drainage capacity of the drainage system and altering the confluence of runoff. Under the control of these operation strategies, flooding can be abated, infrastructure stability can be improved, and the operational cost can be significantly lowered. Furthermore, the TFV reduction efficiency of the multiobjective ISM has better performance for long-duration rainfall events, which means that the ISM may be more suitable for long-duration rainfall events. Therefore, decision-makers should balance multiple objectives, such as flooding, infrastructure stability, and operational costs, when choosing an optimal strategy. However, flooding is not completely eliminated via ISM control, implying that ISM may only mitigate flooding due to the limited capacity of the drainage system. The observed rainfall scenarios verified that the strategies generated by the ISM could effectively reduce the TFV, improve infrastructure stability, and decrease operational costs compared to the current operation rule.

## **4.2 Best strategy under changing conditions**

### **4.2.1 Influence of climate change on rainfall and flooding**

In the climate change scenarios, flooding and operational costs are greater than those in the baseline scenario and increase with rainfall intensity. Flooding uncertainty stemming from various sources also increased as the rainfall intensified. Previous studies have proven that the major uncertainty sources of hydrological modelling are hydrological model parameters, GCMs, and emission scenario uncertainties (Galavi and Mirzaei 2020; Galavi et al. 2019). The increased flooding and boosted operational costs associated with climate change indicate the extreme urgency of adopting suitable strategies to resist climate change damage.

### **4.2.2 Climate change mitigation and local adaptation strategies**

Given flooding, infrastructure stability, and cost, infrastructure upgrading strategies are only suitable for small rainfall events that lack sufficient flexibility to adapt to changing circumstances (Zhou, 2014). The performance of infrastructure upgrading strategies is better than that of simplified LID strategies in mitigating urban flooding (Fig. 3 and Fig. 4). Better adapted LID strategies have a minimal impact on urban flood reduction, while reduction of flooding based on infrastructure upgrading strategies decrease significantly. The simplified LID strategies could potentially reduce TFV, lower water level fluctuation, and lower the operational cost of the facility. However, the

material and construction costs of the LID strategies are much greater (Joshi et al. 2021). In addition, more investment in the LID strategies does not mean better performance (Leng et al. 2021). Therefore, a holistic evaluation of LID performance under various rainfall intensities and LID scales must be studied. The climate change mitigation strategy performs worst in mitigating urban floods and reducing operational costs, which indicates that it is urgent to adopt an adaptation strategy to reduce urban flood disasters.

By comparing the control effect of TFV, infrastructure stability, operational costs and flooding at specific nodes between various strategies, the ISM outperformed, and the climate change mitigation strategy fared worst. However, the potential of the ISM is constrained by the limitations of the storage and conveyance capacity of the drainage system (Lund et al. 2020). For example, suppose the urban flood wants to be eliminated. In that case, the intelligent scheduling model must be integrated with other solutions to boost the underground capacity, such as enlarging drainage infrastructure or applying the LID strategies (Zhou, 2014).

In general, the ISM-based strategy is the most efficient and economically optimal one among climate change mitigation and local adaptation strategies; it alters the confluence of runoff by utilizing the storage and conveyance capacity of drainage systems. The results show that the designed intelligent scheduling model in the simulation-optimization framework can mitigate



urban flooding under future climate change.

## 5. Conclusions

In this study, an efficient simulation-optimization intelligent scheduling model based on multiobjective particle swarm optimization is proposed to mitigate the flooding volume of urban drainage systems; this model alters the confluence of runoff by utilizing the storage and conveyance capacity of the drainage system. To achieve this, the SWMM is coupled with a multiobjective optimization algorithm to optimize and evaluate the strategies generated by ISM. Unlike the existing operation model that focuses only on local overflows of drainage systems, the proposed model incorporates the global overflow of drainage systems, infrastructure stability, and operation costs into the scheduling process to produce more accurate results and help the model evaluate overflows of urban flooding. Based on observed historical rainfall events and synthetic rainfall events generated by the Gumbel distribution, the proposed ISM is an effective model that can mitigate the total flood volume, improve infrastructure stability, and lower operational costs. In addition, the performance of the proposed model is verified by comparing it with other climate change adaptation strategies and climate change mitigation strategies, which perform best among climate change mitigation and adaptation strategies.

This study recommends coupling the ISM with the LID as a promising strategy to realize complementary source control and terminal governance, handle further excess stormwater caused by heavy storms, ensure the stability of drainage infrastructure, and save total costs. The results of this study provide an extensive and reliable comparison of multiple benefits and diverse strategies under variable conditions.

## Appendix

### C1. The constraint of the multiobjective functions

When optimizing the operation of the urban drainage system, the following constraints should be considered as:

The level for turning off each pump is lower than the level for turning it on:

$$0 \leq WL_{1,r} \leq H_{\max}$$

$$0 \leq WL_{2,r} \leq WL_{1,r}$$

Pump discharge limits:

$$Q_{i,t} = \begin{cases} 0 & h_t < WL_{2,r} \\ \sum_{r=1}^M z Q_{\text{pump},r} & WL_{2,r} < h_t < WL_{1,r} \\ \sum_{r=1}^M Q_{\text{pump},r} & h_t > WL_{1,r} \end{cases}$$

Opening settings of weir (e) limits:

$$0 \leq e \leq 1$$

where  $WL_{1,r}$ ,  $WL_{2,r}$  represents the front-pool water depth at which pump  $r$  is turned on and off, respectively;  $H_{\max}$  represents the maximum front-pool

water level;  $Q_{i,t}$  represents the discharge of pump station  $i$ ;  $h_t$  represents the water depth;  $M$  represents the number of pump;  $Q_{\text{pump},r}$  represents the capacity of pump  $r$ ;  $z$  is equal to 1 when the pump has been turned on, otherwise is 0.

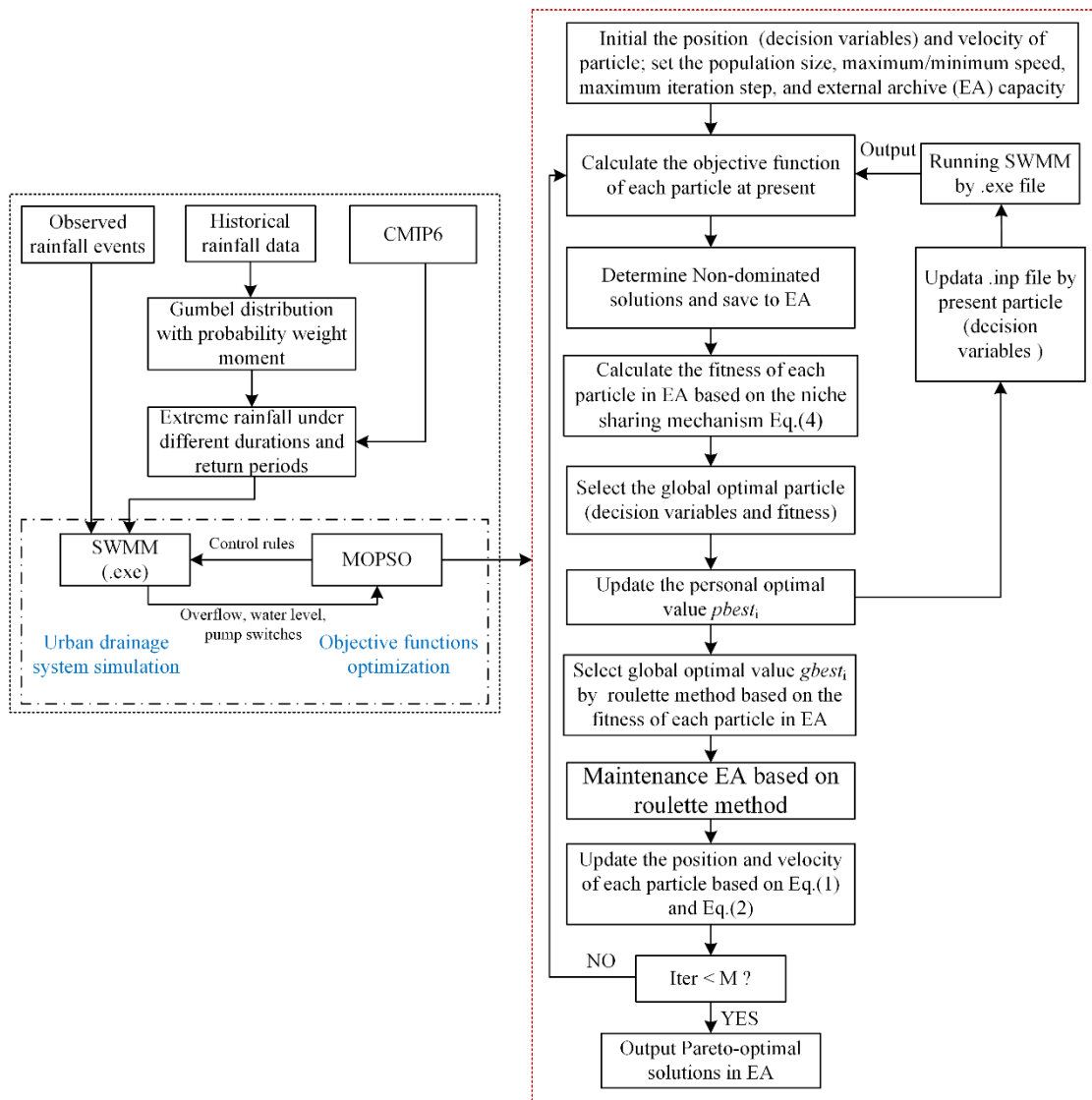


Fig. A1. The simulation-optimization framework.

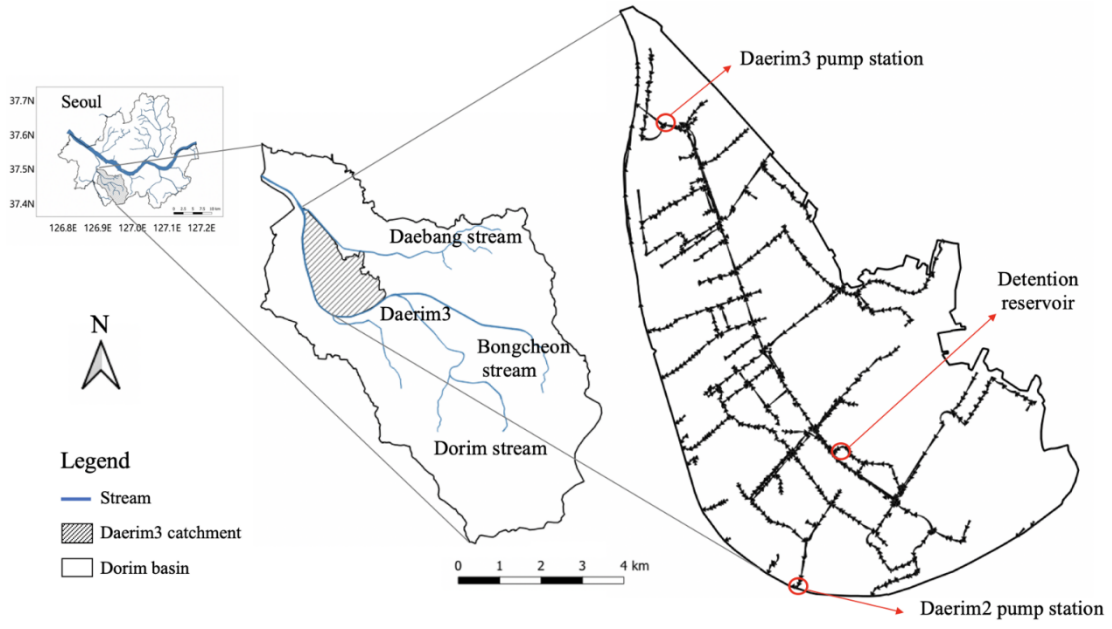


Fig. A2. Location of the Dorim basin, South Korea.

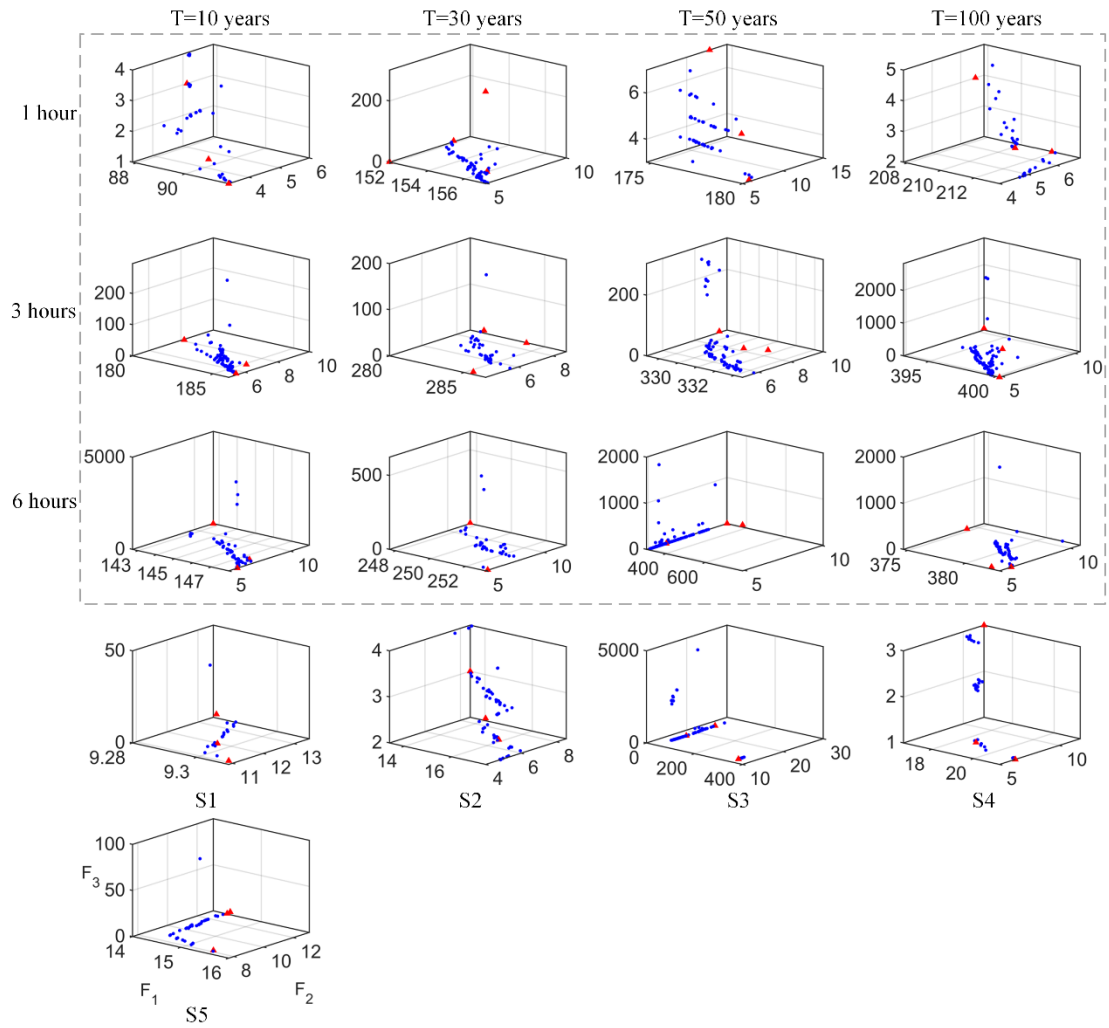


Fig. A3. The Pareto solutions of the designed ISM under the design rainfall events ( $T=10, 30, 50, 100$ ) and historical rainfall scenarios (referred to Table S1).

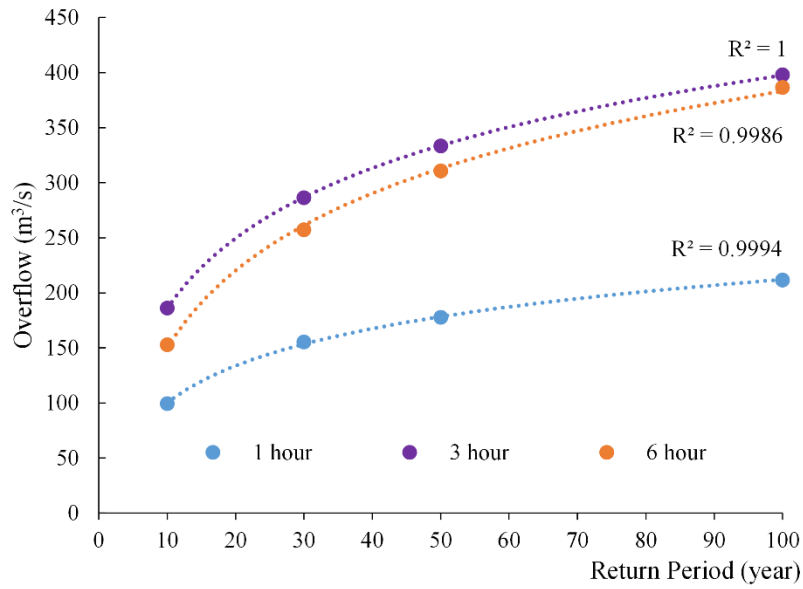


Fig. A4. The relationship between the flooding (TFV) and rainfall intensity expressed as return period (Log-linear relationship).

Table A1. Detailed information for the components of SWMM model.

Component	Number	Capacity
Detention reservoir	1	2447 m <sup>3</sup>
Daerim2 pump station	1	1.8667 m <sup>3</sup> /s per pump × 3
Daerim3 pump station	1	4.17 m <sup>3</sup> /s per pump × 10
Daerim DR pump station	1	0.15 m <sup>3</sup> /s per pump × 2
Weir	1	/
Conduits	673	/
Nodes	626	/
Sub-catchments	529	/

## Acknowledgments

This work was supported by National Natural Science Foundation of China

(52009092).

This is also a collaborative research achievement of the Smart Water Institute (SWI) and Seoul Institute of Technology (SIT) supported by the Seoul Institute of Technology (2021-AB-008), Seoul, South Korea.

## Declarations

**Ethical Approval** Not applicable.

**Consent to Participate** Not applicable.

**Consent to Publish** Not applicable.

**Competing Interests** Not applicable.

## References

- Bi X, Wang C (2018) A niche-elimination operation based NSGA-III algorithm for many-objective optimization. *Applied Intelligence*, 48(1), 118-141. doi:10.1007/s10489-017-0958-4
- Das I, Dennis JE (1997) A closer look at drawbacks of minimizing weighted sums of objectives for Pareto set generation in multicriteria optimization problems. *Structural optimization*, 14(1), 63-69.
- Feng M, Jung K, Li F et al (2020) Evaluation of the Main Function of Low Impact Development Based on Rainfall Events. *Water*, 12(8). doi:10.3390/w12082231
- Galavi H, Kamal MR, Mirzaei M et al (2019) Assessing the contribution of different uncertainty sources in streamflow projections. *Theoretical and Applied Climatology*, 137(1), 1289-1303. doi:10.1007/s00704-018-2669-0
- Galavi H, Mirzaei M (2020) Analyzing Uncertainty Drivers of Climate Change Impact Studies in Tropical and Arid Climates. *Water Resources Management*, 34(6), 2097-2109. doi:10.1007/s11269-020-02553-0
- García L, Barreiro-Gomez J, Escobar E et al (2015) Modeling and real-time control of urban drainage systems: A review. *Advances in Water Resources*, 85, 120-132. doi:<https://doi.org/10.1016/j.advwatres.2015.08.007>
- Ghodsí SH, Zahmatkesh Z, Goharian E et al (2020) Optimal design of low impact development practices in response to climate change. *Journal of Hydrology*, 580, 124266. doi:<https://doi.org/10.1016/j.jhydrol.2019.124266>

- Hsu NS, Huang CL, Wei CC (2013) Intelligent real-time operation of a pumping station for an urban drainage system. *Journal of Hydrology*, 489, 85-97. doi:<https://doi.org/10.1016/j.jhydrol.2013.02.047>
- Huff FA (1967) Time distribution of rainfall in heavy storms. *Water Resources Research*, 3(4), 1007-1019. doi:<https://doi.org/10.1029/WR003i004p01007>
- Jafari F, Mousavi SJ, Yazdi J et al (2018) Real-Time Operation of Pumping Systems for Urban Flood Mitigation: Single-Period vs. Multi-Period Optimization. *Water Resources Management*, 32(14), 4643–4660.
- Joshi P, Leitão JP, Maurer M et al (2021) Not all SuDS are created equal: Impact of different approaches on combined sewer overflows. *Water Research*, 191, 116780. doi:<https://doi.org/10.1016/j.watres.2020.116780>
- Kennedy J, Eberhart R (1995) Particle Swarm Optimization[C]//Proceedings of the IEEE International Conference on Neural Networks.
- Lee JH, Yuk GM, Moon HT et al (2020) Integrated Flood Forecasting and Warning System against Flash Rainfall in the Small-Scaled Urban Stream. *Atmosphere*, 11(9), 971.
- Lee T, Son C, Kim M et al (2020) Climate Change Adaptation to Extreme Rainfall Events on a Local Scale in Namyangju, South Korea. *Journal of Hydrologic Engineering*, 25(5), 05020005. doi:10.1061/(ASCE)HE.1943-5584.0001906
- Leng L, Jia H, Chen AS et al (2021) Multi-objective optimization for green-grey infrastructures in response to external uncertainties. *Science of The Total Environment*, 775, 145831. doi:<https://doi.org/10.1016/j.scitotenv.2021.145831>
- Liu DS, Tan KC, Goh CK et al (2006) On Solving Multi-objective Bin Packing Problems Using Particle Swarm optimization. *IEEE International Conference on Evolutionary Computation*, 2095-2102. doi: 10.1109/CEC.2006.1688565.
- Lund NSV, Borup M, Madsen H et al (2020) CSO reduction by integrated model predictive control of stormwater inflows: a simulated proof of concept using linear surrogate models. *Water Resources Research*, 56(8), e2019WR026272. doi:<https://doi.org/10.1029/2019WR026272>
- Lund NSV, Borup M, Madsen H et al (2019) Integrated stormwater inflow control for sewers and green structures in urban landscapes. *Nature Sustainability*, 2(11), 1003-1010. doi:10.1038/s41893-019-0392-1
- Mahmoud SH, Gan TY (2018) Urbanization and climate change implications in flood risk management: Developing an efficient decision support system for flood susceptibility mapping. *Science of The Total Environment*, 636, 152-167. doi:<https://doi.org/10.1016/j.scitotenv.2018.04.282>
- Meng F, Fu G, Butler D (2020) Regulatory Implications of Integrated Real-Time Control Technology under Environmental Uncertainty. *Environmental Science & Technology*, 54(3), 1314-1325. doi:10.1021/acs.est.9b05106
- Mostaghim S, Teich J (2003). Strategies for finding good local guides in multi-objective particle swarm optimization (MOPSO). Paper presented at the Proceedings of the 2003 IEEE Swarm Intelligence Symposium. SIS'03 (Cat. No.03EX706) (pp. 26–33).



IEEE.

- Ngo TT, Yoo DG, Lee YS et al (2016) Optimization of Upstream Detention Reservoir Facilities for Downstream Flood Mitigation in Urban Areas. *Water*, 8(7): 290. doi:10.3390/w8070290
- Qin Hp, Li ZX, and Fu G (2013) The effects of low impact development on urban flooding under different rainfall characteristics. *Journal of Environmental Management*, 129, 577-585. doi:https://doi.org/10.1016/j.jenvman.2013.08.026
- Rathnayake U, Anwar A (2019) Dynamic control of urban sewer systems to reduce combined sewer overflows and their adverse impacts. *Journal of Hydrology*, 579, 124150-.
- Rossman LA (2009) US EPA SWMM 5.0 User's Manual EPA/600/R-05/040. Water Supply and Water Resources Division, National Risk Management Research Laboratory, Cincinnati, USA.
- Ryu J, Lee H, Yu S et al (2014) Statistical evaluation on storm sewer design criteria under climate change in Seoul, South Korea. *Urban Water Journal*, 11(5), 370-378. doi:10.1080/1573062X.2013.801498
- Sadler JM, Goodall JL, Behl M et al (2019) Leveraging open source software and parallel computing for model predictive control of urban drainage systems using EPA-SWMM5. *Environmental Modelling & Software*, 120, 104484. doi:https://doi.org/10.1016/j.envsoft.2019.07.009
- Sun C, Romero L, Joseph-Duran B et al (2020) Integrated pollution-based real-time control of sanitation systems. *Journal of Environmental Management*, 269, 110798. doi:https://doi.org/10.1016/j.jenvman.2020.110798
- Wang X, Tian W, Liao Z (2021) Offline Optimization of Sluice Control Rules in the Urban Water System for Flooding Mitigation. *Water Resources Management*, 35(3), 949-962. doi:10.1007/s11269-020-02760-9
- Wong BP, Kerkez B (2018) Real-Time Control of Urban Headwater Catchments Through Linear Feedback: Performance, Analysis, and Site Selection. *Water Resources Research*, 54(10), 7309-7330. doi:https://doi.org/10.1029/2018WR022657
- Yang J, Zhou J, Liu L et al (2009) A novel strategy of pareto-optimal solution searching in multi-objective particle swarm optimization (MOPSO). *Computers & Mathematics with Applications*, 57(11), 1995-2000. doi:https://doi.org/10.1016/j.camwa.2008.10.009
- Yang SN, Lcc A, Fjc B (2019) AI-based design of urban stormwater detention facilities accounting for carryover storage. *Journal of Hydrology*, 575, 1111-1122.
- Yazdi J, Choi HS, Kim JH (2016) A methodology for optimal operation of pumping stations in urban drainage systems. *Journal of Hydro-environment Research*, 11, 101-112. doi:https://doi.org/10.1016/j.jher.2015.09.001
- Zhou Q (2014) A Review of Sustainable Urban Drainage Systems Considering the Climate Change and Urbanization Impacts. *Water*, 6(4). doi:10.3390/w6040976
- Zhou Q, Leng G, Huang M (2018) Impacts of future climate change on urban flood volumes in Hohhot in northern China: benefits of climate change mitigation and adaptations.

Zhou Q, Leng G, Su J et al (2019) Comparison of urbanization and climate change impacts on urban flood volumes: Importance of urban planning and drainage adaptation. *Science of The Total Environment*, 658, 24-33. doi:<https://doi.org/10.1016/j.scitotenv.2018.12.184>

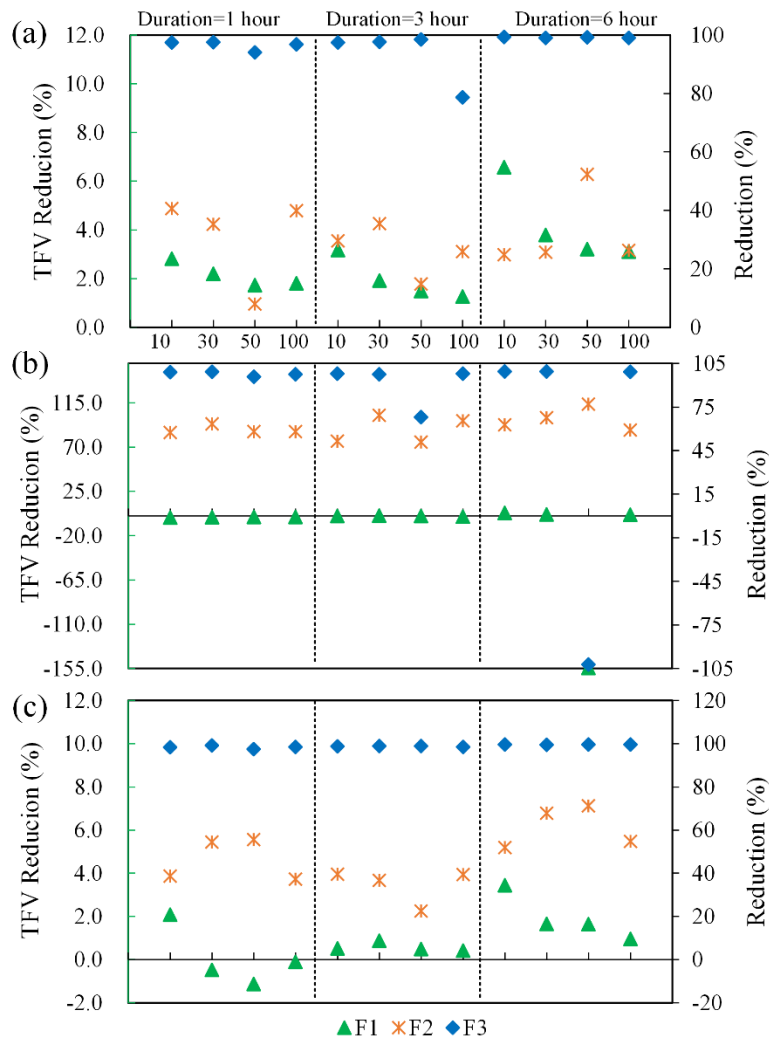


**Fig. 1.** The flooding (TFV), water level fluctuation and operational cost reduction of (a) the strategy with a minimum TFV, (b) the strategy with a minimum water level fluctuation, and (c) the strategy with a minimum operational cost generated by the designed ISM for different rainfall durations and return periods.

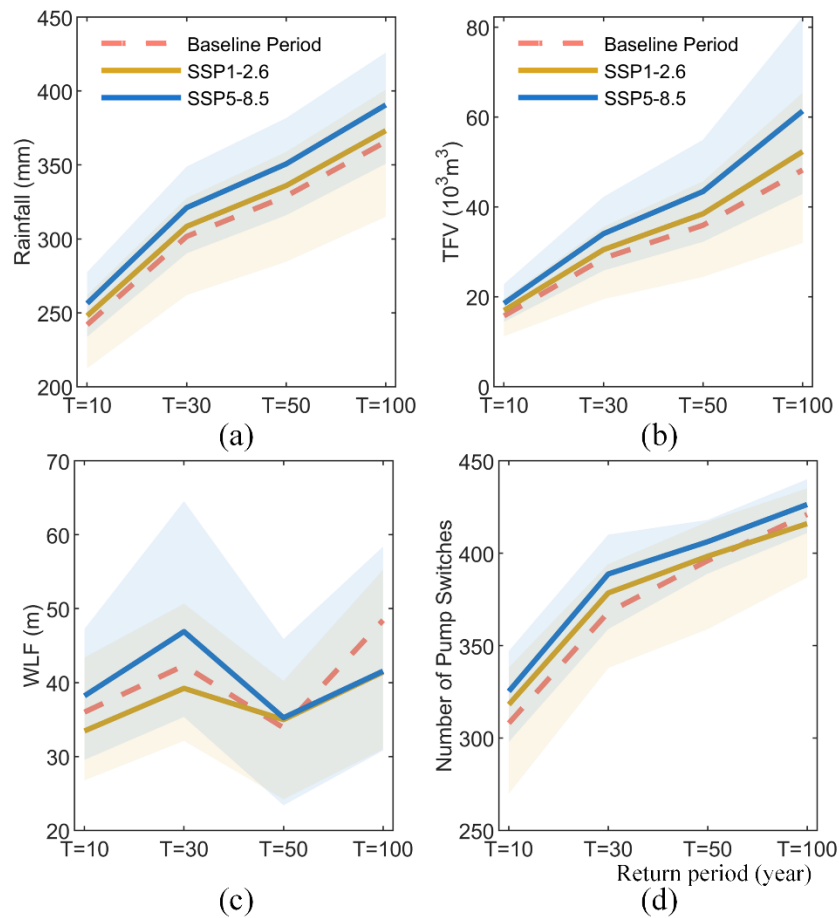


**Fig. 2. The (a) rainfall, (b) flooding (TFV), (c) water level fluctuation, and (d) operational cost under the synthetic rainfall events with different return periods for baseline period (1961-2018) and future climate change scenarios.**

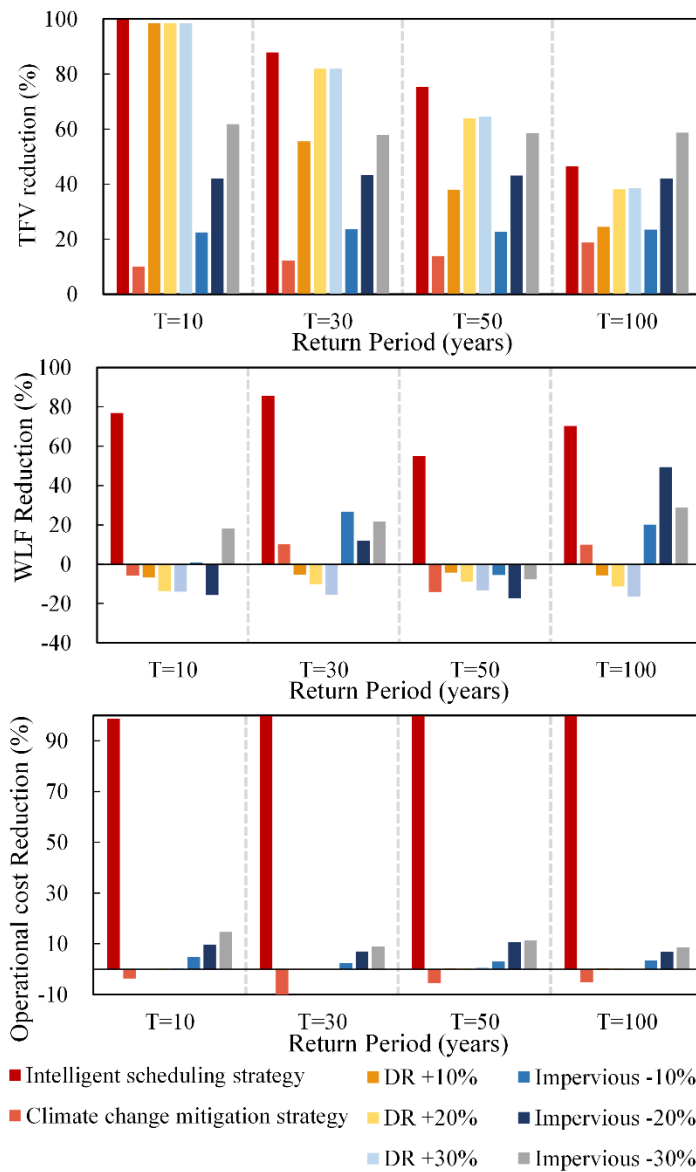


**Fig. 3. Comparison the flooding (TFV), water level fluctuation and operational cost reduction for different strategies (DR +10%: represents detention reservoir with a volumetric extension of 10%; Impervious -10%: represents the impervious surface ratio with a reduction of 10%) under different synthetic rainfall scenarios (T=10, 30, 50, and 100 years).**

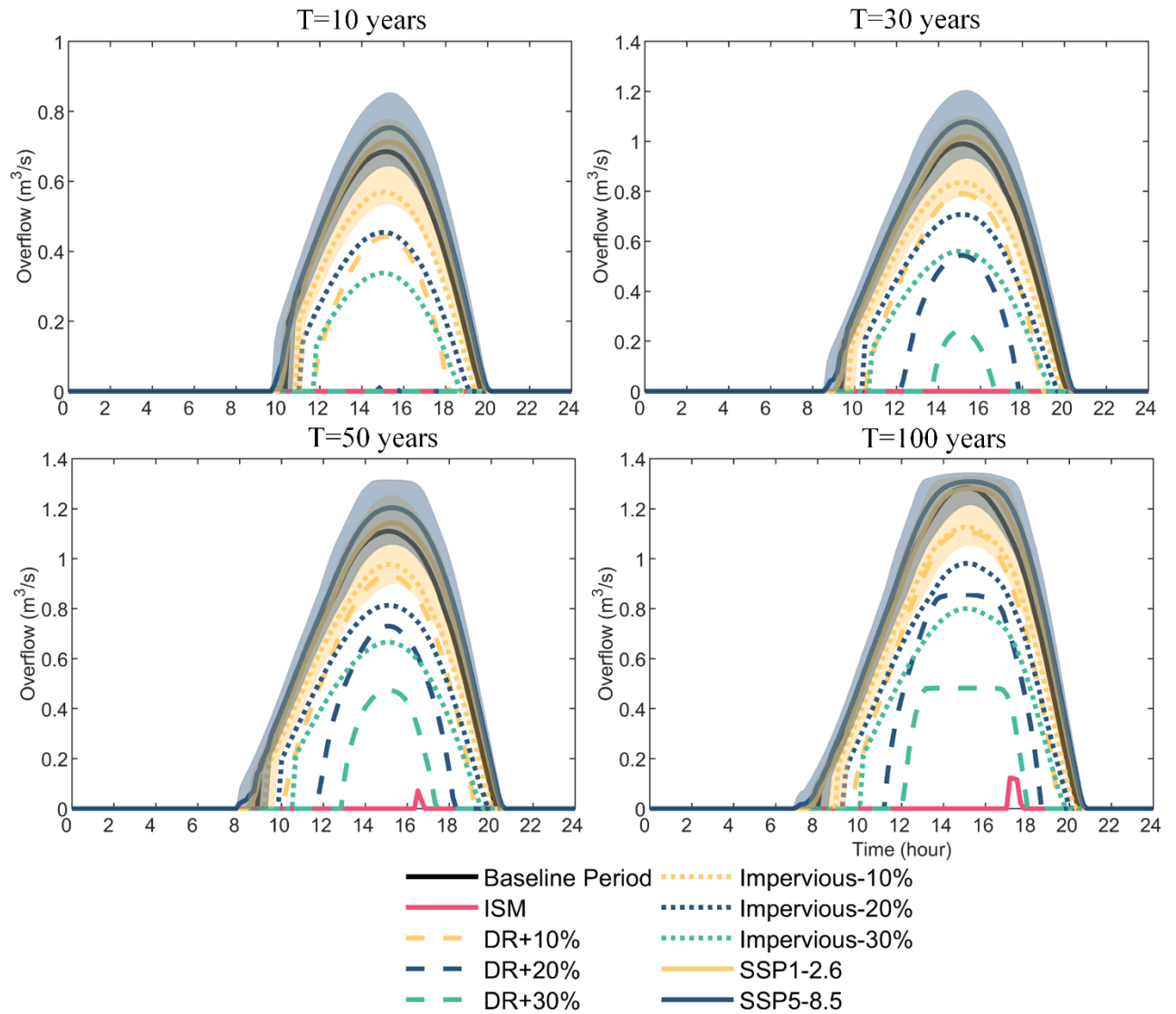


**Fig. 4.** Flooding at system nodes MH23446 for different strategies (DR +10%: represents detention reservoir with a volumetric extension of 10%; Impervious -10%: represents the impervious surface ratio with a reduction of 10%) under different synthetic rainfall scenarios (T=10, 30, 50, and 100 years).